Critical behavior of a ternary microemulsion studied by turbidity, density, and refractive index

Y. Jayalakshmi
Service de Physique des Atomes et des Surfaces, Centre d'Etudes de Saclay, F-91191 Gif-sur-Yvette CEDEX, France

D. Beysens
Service de Physique de l'Etat Condensé, Centre d'Etudes de Saclay, F-91191 Gif-sur-Yvette CEDEX, France
(Received 22 February 1991)

A detailed study of turbidity, density, and refractive index in the critical region of two samples of a water in an oil ternary microemulsion system, water plus benzene plus benzyl hexadecyl dimethylammonium chloride (BHDC), is presented. Special care is taken to determine the criticality of the samples. The critical point is approached from the homogeneous phase by varying the temperature at fixed concentrations of the components. Along this path Fisher-renormalized Ising exponents are expected. The critical exponents for the correlation length (ν) and osmotic susceptibility (γ) are determined through the turbidity. The critical exponent α can be deduced from the $(1-\alpha)$ behavior of the density and the refractive index. From mere numerical analysis alone turbidity behavior cannot be distinguished between Ising and Fisher-renormalized Ising exponents. However, physical arguments suggest the latter values for the exponents ν and γ. We do not see any anomaly in the density within a resolution of $\pm 3\times 10^{-6}$. This is consistent with the renormalization of α $[\alpha^*=-\alpha/(1-\alpha)]$. A very weak anomaly in the refractive index is detected which is better described by a function of the exponential type, which has been discussed for a quaternary microemulsion near the critical end point, than the $(1-\alpha)$ power behavior.

PACS number(s): 82.70.−y, 64.70.−p, 78.20.−e

I. INTRODUCTION

Microemulsion systems exhibit complex phase behavior with several critical points in their phase diagram [1]. Their critical behavior is expected to be similar to gas-liquid systems and hence should show three-dimensional (3D) Ising exponents [2]; this question has attracted considerable interest in the recent past [3–10]. In multicomponent mixtures a critical point can be approached through several thermodynamic paths and the exponents are shown to depend on the thermodynamic path of approach [11]. For a ternary water-in-oil (WO) microemulsion, with temperature (T) and water-to-surfactant ratio (W/S) acting as field variables, a critical point in the phase diagram can be approached either by varying W/S at fixed T and the oil concentration or by varying T at the fixed overall concentrations of the components [4]. For the former path, Ising exponents are expected according to the arguments developed by Griffiths and Wheeler [11]. The latter path with T as the variable poses the double density constraints of fixing both the oil and water concentrations. Along such paths the exponents are shown to be stronger and are Fisher renormalized in the asymptotic limit [12]. For example, the exponents for the correlation length (ν), osmotic compressibility (γ), and specific heat (α) renormalize as $\nu^*=\nu/(1-\alpha)$, $\gamma^*=\gamma/(1-\alpha)$, and $\alpha^*=-\alpha/(1-\alpha)$. The negative α^* implies that the specific heat will remain finite instead of diverging. This has similar consequences on the derived properties such as the density (ρ) and refractive index (n). The expected $(1-\alpha)$ anomaly in ρ and n would renormalize as $1/(1-\alpha)$, indicating that there is no anomaly. Light-scattering experiments on the ternary microemulsion water plus decane plus sodium bis(2-ethylhexyl)sulfosuccinate (aerosol OT or AOT) (WDA) show the expected Fisher-renormalized value ν^* [3,4,8]. But a very small anomaly was detected in the refractive index in an independent study [7] and was analyzed as a $(1-\alpha)$ behavior. This contradiction may be due to the uncertainties involved in detecting the very weak anomalies. In fact, in binary liquid mixtures, there is only one single report of an intrinsic n anomaly [13], but it has not been confirmed in an independent study [14] on the same system and may possibly be an artifact of the method of the data analysis [15].

On the other hand, the quaternary microemulsion water plus dodecane plus sodium dodecyl sulfate (SDS) plus pentanol (WDSP) has shown non-Ising behavior at the critical points close to a critical end point (CEP) [5,6,10]. In the vicinity of the CEP, this system phase separated into complex coexisting phases such as the spongy microemulsion and lamellar phases. The observed refractive-index anomaly near CEP [6,10] was consistent with a model based on the chemical modifications in the microemulsion phase, as a pretransitional effect leading to the changes in the volume fraction of the dispersed phase. This was shown to change n at a constant average density. It is interesting to address the same question for a three-component microemulsion to check the universality of this behavior.

Our study on the ternary microemulsion water plus benzene plus benzyl hexadecyl dimethylammonium chloride (BHDC) [with the chemical formula $C_{16}H_{33}$-$(C_6H_5)N^+(CH_3)_2Cl^-$] (WBB) was motivated by

 ©1992 The American Physical Society

the above questions of the critical exponents for these complex systems. Since in these systems very small changes in the concentrations of the components modify the phase diagram considerably, comparison of the various exponents is possible only when they are measured on the same sample. We have measured the turbidity τ, density ρ, and refractive index n for a fixed value of W/S and of the benzene concentration and varying T. The data can be fitted to Ising or to Fisher-renormalized Ising exponents. We did not see any critical anomaly in ρ within our experimental resolution. A very weak anomaly was observed in n. This anomaly is fitted better by the exponential function that has been discussed for the four-component microemulsion WDSP [6,10] near the CEP than by a power-law function with $(1-\alpha)$ as the exponent.

II. CRITICAL BEHAVIOR OF τ, ρ, AND n

The turbidity τ corresponds to the attenuation of light in the sample. It is proportional to the intensity of the scattered light per unit length of the sample integrated over all the angles [16]. Using the Ornstein-Zernike form for the scattered intensity in the critical region, τ can be written as

$$\tau = A_0 \pi \chi_T G(z) , \tag{1}$$

where

$$A_0 = (\pi^2/\lambda^4)\rho \left[\frac{dn^2}{dx} \right]_T^2 k_B T .$$

χ_T is the static osmotic susceptibility; $z=2(k_0\xi)^2$, where ξ is the correlation length with the amplitude ξ_0, k_0 is the incident wave vector, and $k_0 = 2\pi n/\lambda_0$. Here x is the concentration of one of the components and λ_0 is the wavelength of light in vacuum. The function $G(z)$ is

$$G(z) = \frac{(2z^2+2z+1)\ln(1+2z)}{z^3} - \frac{2(1+z)}{z^2} . \tag{2}$$

The scaling forms for χ_T and ξ are

$$\chi_T = \chi_T^0 t^{-\gamma}(1+a_\chi t^\Delta + \cdots) , \tag{3}$$

$$\xi = \xi_0 t^{-\nu}(1+a_\xi t^\Delta + \cdots) , \tag{4}$$

where a_χ and a_ξ are the coefficients of the leading term in the nonanalytic corrections (NAC's) to χ_T and ξ, respectively, and $\Delta = 0.5$ is the exponent for the NAC's. Using Eqs. (3) and (4), τ can be written in the asymptotic limit as

$$\tau = \tau_0(1+t)t^{-\gamma}G(z) , \tag{5}$$

$$z = 2(k_0\xi_0)^2 t^{-2\nu} . \tag{6}$$

Here $\tau_0 = A_0 \pi \chi_T^0$ and $t=(T-T_c)/T_c$. Fitting the turbidity data by Eq. (5) with Eqs. (2) and (6) yields the exponents γ and ν and the correlation-length amplitude ξ_0. The exponent γ is determined from the data corresponding to small $k_0\xi$, i.e., far from the critical point.

The mass density ρ and specific heat are related through the thermodynamic relation

$$C_{P,x_c} - C_{v,x_c} = \left[\frac{d\rho}{dt} \right]_{P,x_c} \Big/ \left[\rho^2 \left[\frac{dT}{dP} \right]_{v,x_c} \right] , \tag{7}$$

where P is the pressure, v is the volume, and x_c is the critical concentration. As t approaches zero, C_{v,x_c} rounds off, $(dT/dP)_{v,x_c}$ takes the limiting value dT_c/dP along the critical line, and C_{P,x_c} diverges with the α exponent ($\alpha = 0.11$). Therefore the asymptotic behavior of ρ comes from that of C_{P,x_c}:

$$C_{P,x_c} = C_{P,x_c}^b + (Ak_B/\alpha)t^{-\alpha}(1+a_{c_P}t^\Delta + \cdots) . \tag{8}$$

Here k_B is the Boltzman constant, C_{P,x_c}^b is the background specific heat, and a_{c_P} is the amplitude of the first NAC term. Substituting Eq. (8) in Eq. (7), ρ can be written in the asymptotic limit as

$$\rho = \rho^b + \left[Ak_B \left[\frac{\rho_c^2 dT_c}{dP} \right] \Big/ \alpha(1-\alpha) \right] t^{1-\alpha} . \tag{9}$$

Here the superscript b stands for the background terms and the subscript c for the parameter values at the critical temperature T_c. The parameter A is given by the two-scale-factor universality, which connects the leading amplitudes of the critical terms. Here one makes use of the relation [17]

$$R_{\xi^+} = A^{1/3}\xi_0 , \tag{10}$$

where $R_{\xi^+} = 0.27$ is universal. Since ξ_0 for the microemulsions is of the order of 20–30 Å, the specific heat, and hence the density anomaly, is expected to be three orders of magnitude smaller than that in liquid mixtures and could only be detected with very-high-precision data.

However, under Fisher renormalization of the exponents, C_{P,x_c} is finite at T_c and in this case the obvious extension of Eq. (9) in which α is replaced by α^* is not adequate.

The refractive index is related to the density through the extended Lorentz-Lorenz formula (LL) [18]

$$\frac{(n^2-1)}{(n^2+2)} = \frac{4\pi}{3}\rho\theta_0(1+F)^{-1} , \tag{11}$$

where θ_0 is the mixture average molecular polarizability and F is the correction to the LL formula, due to local field effects. Equation (11) gives

$$\frac{dn}{dt} = \frac{1}{\rho}\frac{d\rho}{dt}\frac{(n^2-1)(n^2+2)}{6n}\left[1 + \frac{\rho}{1+F}\frac{\frac{dF}{dt}}{\frac{d\rho}{dt}} \right] . \tag{12}$$

Therefore, in the absence of F, the behavior of n is completely determined by that of ρ. In noncritical fluids F contributes to a -10% background correction for $(dn/dt)_{\rm LL}$, which is the calculated value of dn/dt from LL formula [19]. In critical fluids F is expected to exhibit in addition a $(1-\alpha)$ behavior [20].

III. EXPERIMENTAL PROCEDURE

The three-component microemulsion system water plus benzene plus BHDC (WBB) was used for the study. The studied samples had upper critical-solution temperatures. The complete phase diagram of this system is not known. Two stock solutions of samples (named A and B) [21], prepared in two different laboratories, were used. The compositions were (in weight percentages)

	A (%)	B (%)
benzene	87.415	90.900
BHDC	4.373	3.045
water	8.212	6.055

Note that the W/S ratios for the two samples were fairly close to each other. Sample B was supplied in a glass tube with a thin Teflon seal, and sample A was contained in a flame-sealed glass ampule. Since benzene boils at 80 °C, care was taken to avoid its evaporation while filling the sample. Sample B (sets 1 and 2) was filled first into a special cell designed and calibrated for the simultaneous measurement of ρ, n, and τ [14]. Sets 1 and 2 of sample B correspond to different masses of the liquid. Set 3 of sample B was specially filled for n and τ measurements in a thin cell. Sample A was filled into two cells and were named as sets 4 and 5. The cells were sealed by the Teflon-screwed Rotaflo cap. Thorough mixing of the samples was assured by scanning the laser beam for gradients. Several small runs (named $a,b,c,\ldots$) within a set were made to ascertain the equality of the remixed samples to the original ones. Table I gives the complete details of all the runs [22]. Here L is the path length for the laser beam in the cell. $L=2$ and 5 cm correspond to the same cell in two mutually perpendicular positions. From Table I we see that there is a considerable difference between the T_c's of different sets. Though we do not know the exact reason for this effect, it is not very surprising as it is known that small changes in the concentration of the components change T_c considerably in these systems (see Table I of Ref. [4]). Such small changes in the concentration can occur during manipulations, especially when benzene is one of the components. Hence different sets of a given sample may not correspond to the same critical point in the phase diagram. Therefore each set is independently checked for criticality, according to a procedure described later, and analyzed independently.

Sample turbidity was determined by measuring the transmitted beam intensity through the sample using the formula

$$\tau=-\frac{1}{L}\ln\left[\frac{I_T}{I_0}\right], \tag{13}$$

where I_T and I_0 are the transmitted intensities with and without the cell, respectively. The transmission losses due to the cell windows corresponded to a turbidity correction of $(-1/L)\times 0.005\ \mathrm{cm}^{-1}$, which was within the resolution for all the L values used. By comparing the τ data at different L, we could not see any effect of multiple scattering close to T_c. The precision of τ was $0.03\ \mathrm{cm}^{-1}$ for $L=5$ cm, 2 cm, and $0.1\ \mathrm{cm}^{-1}$ for $L=0.2$ cm. We consider set 4 of sample A as the most accurate set for τ.

The height $H(T)$ of the sample expanding in a calibrated narrow capillary tube (diameter $\phi=0.1$ cm) was measured at each temperature T by measuring the positions of the meniscus $X(T)$ and a fiducial mark X_0. The density was calculated using the cell-calibration parameters [14]

$$\rho(T)=M\{V_0+(\pi\phi^2/4)[H(T)+H']\}^{-1}\ ,$$
$$H(T)=X(T)-X_0\ ,\quad H'=X_0-X'=3\ \mathrm{cm}\ , \tag{14}$$

TABLE I. Details of all the runs on two samples (B and A) for the microemulsion WBB.

Sample	L (cm)	T_c Set (runs)	(°C)	Temperature range $T-T_c$ (K)	Property
B	5	1	27.166	6–2.3	ρ
	5			6–0.85	τ
	2			0.85–0.002	τ
	2	2(a,b,c)	26.753	3.2–0.005	ρ,τ
	2	2(d,e)	26.748	0.4–0.003	ρ,τ
	5	2(f)	26.748	0.84–23.3	τ
	5	2(f)	26.748	0.84–3.14	ρ
	0.2	3(a,b,c,d)	24.664	1.88–0.001	τ
		3(a,b,c,d)	24.475	29.0–0.001	n
		3(e,f)	24.475	0.075–13.85	τ
A	5	4(a)	31.444	3.7–1.45	ρ,τ
	2	4(a)		1.45–0.002	
	5	4(b)		1.54–27	
	0.5	5	30.969	22–0.001	n,τ

where V_0 is the calibrated bulk volume below X' and ϕ is the capillary diameter. M is the weight of the liquid, which can be measured within an accuracy of 0.1 mg. However, during the sample filling, small drops of the sample liquid fell on the walls of the neck of the cell, which left behind traces of the surfactant outside the expanding liquid volume. This limited the accuracy of M to 10 mg. The absolute accuracy of the density was limited by the precision of M and was 6.5×10^{-4} g. The height measurements had a relative accuracy of 0.005 cm and corresponded to a relative precision of $\pm3\times10^{-6}$ g cm^{-3} in density.

The refractive index n was obtained by a two-beam-interferometer technique described elsewhere [23]. Change in n between two temperatures (Δn) is related to the shift in fringe order ΔP through

$$\Delta n=\Delta P\lambda_0/2L \ , \tag{15}$$

with $\lambda_0=6328$ Å (He-Ne laser). A precision of ±0.06 fringe corresponded to $\pm1.0\times10^{-5}$ in Δn for $L=0.2$ cm. Though at the cost of reduced precision, this choice of L was unavoidable because of the high turbidity of these samples, which considerably reduced the contrast of the fringes at large L. A rough estimate gave a fringe contrast of 0.007 for $L=1$ cm and 0.6 for $L=0.2$ cm at 10 mK from T_c.

A. Determination of T_c

The determination of T_c and criticality of microemulsions is nontrivial and is never mentioned in the literature. We measured τ for all the runs. Phase separation was signaled by the slight and slow increase in the transmissivity with time at a fixed temperature. However, when the sample was left at the same temperature, even in our thinnest sample ($L=0.2$ cm), the meniscus was not visible over 25 days for 5 mK below T_c. Since the phase-separation dynamics is governed by the correlation time, which is proportional to ξ^3, phase separation should be extremely slow in systems with large ξ. A typical estimate [24] showed that it should take 69 days for a quench of 5 mk below T_c and 15 h for a quench of 150 mK below T_c for a domain size of 1 cm. Therefore, unlike in binary liquids, one cannot anticipate the appearance of the meniscus close to T_c within the time scale of the experiments.

In order to locate T_c and check the criticality of our samples, we adopted the following procedure. The observation of the meniscus at equal volumes of the separated phases close to T_c was taken as the confirmation of the criticality. The turbidity was measured at different heights of the sample as a function of time at several quench depths until the meniscus was seen by the eye. We observed a minimum in the transmitted intensity for the height corresponding to the center of the sample volume, even within 5 mK below T_c. The transmission minimum remained at the same height through the quenches, and the meniscus appeared at the same height at nearly 150 mK below T_c. We attributed the transmission minimum to the defocusing of the beam between the two forming phases. In order to be able to see the meniscus within a day of the first transmission rise, we had to quench our samples 150 mK below T_c. All those samples which showed the meniscus at equal volumes (within an experimental accuracy of $\pm3\%$) at 150 mk below T_c were considered as critical. Only one sample was noncritical (set 5 of sample A), and we did not use these data for comparison. Since the accuracy of the T_c determination was only ±3 mK, in our analysis, data with $(T-T_c)<5$ mk are not included.

IV. RESULTS

The critical exponents were obtained from the τ, ρ, and n data by making a nonlinear-least-squares fit using the curve-fitting program CURFIT by Bevington [25(a)] with a slight modification for the calculation of the standard deviations [25(b)]. The goodness of fit is judged by χ_ν^2, where

$$\chi_\nu^2=\frac{1}{N-n}\sum_{i=1}^{N}\frac{[Y_i-Y(X_i)]^2}{\sigma_i^2} \ . \tag{16}$$

Here N and n are, respectively, the number of data points and number of adjustable parameters in the fitting functions, Y_i, $Y(X_i)$, and σ_i are the ith value of the experimental data, calculated data, and the uncertainty. In estimating the uncertainty σ_i, the effect of the uncertainty in temperature was ignored for the turbidity, whereas it was taken into account for the density and refractive index. These uncertainties were estimated by an approximate average of the instrument resolutions over all the data points within a set or several similar sets, and these values of σ_T and σ_Y (where Y denotes τ, ρ, or n) were used for all the data points within a set. A temperature difference of 0.65 K is added to all the experimental temperatures to correct for the difference between the experimental quartz thermometer and the actual temperature. The accuracy of this temperature is 0.1 K. In all the fitting, T_c is fixed at the experimentally known values.

A. Turbidity

The turbidity data were fitted by Eq. (5) using Eqs. (2) and (6) with varying constraints on Eq. (5). The results are presented in Table II for sample A and in Table III for sample B.

The main results for the turbidity came from sample A, and we discuss their analysis first. (i) When Eq. (5) was assumed as the fitting function, we got ν and γ, close to the mean-field values (fit τ-1: $\nu=0.52\pm0.01$, $\gamma=0.91\pm0.02$). (ii) When a constant background term (τ_b) was added to Eq. (5) as

$$\tau=\tau_0(1+t)t^{-\gamma}G(z)+\tau_b \ , \tag{17}$$

the analysis gave the Ising exponent for ν (fit τ-2: $\nu=0.63\pm0.07$, $\gamma=1.14\pm0.15$). The fit is better as indicated by a better χ_ν^2. The necessity of such a background term is discussed in the work by Rouch *et al.* [8]. It arises from the appreciable single-particle scattering as a result of the large size of the micelles, which is the main

TABLE II. Results of the fits for turbidity data for set 4 of sample A. $\sigma_\tau=0.03$ cm^{-1}; the $(T-T_c)$ range is 27 K. In all the tables, the parameter values inside the parentheses are imposed in these fits. $\Delta=0.5$ [27]. An asterisk indicates the fit we judge best.

Fit	Equation	$10^3(\tau_0\pm\sigma_{\tau_0})$ (cm^{-1})	$\gamma\pm\sigma_\gamma$	$\xi_0\pm\sigma_{\xi 0}$ (Å)	$\nu\pm\sigma_\nu$	As defined (cm^{-1})	χ_ν^2
τ-1	(5)	13±1	0.91±0.02	38.1+0.7	0.52+0.01		0.81
τ-2	(17)	4.8±2.8	1.14±0.15	30.6±3	0.63±0.07	$\tau_b=0.13\pm0.06$	0.75
τ-3		4.9±0.1	1.141±0.002	30.7±0.7	(0.625)	$\tau_b=0.13\pm0.01$	0.75
τ-4		3.2±0.1	(1.24)	27.5±0.7	0.6707± 0.0009	$\tau_b=0.17\pm0.01$	0.76
τ-5	(18)	5.3±2.4	1.142±0.008	32.6±10.2	(0.625)	$\tau_b=0.15\pm0.14$ $a_\chi=-(0.6\pm3)$	0.75
τ-6	(19)	2.3±2.5	1.29±0.25	23.5±6	0.70±0.12	$\tau_{b1}=1.3\pm1.2$ $\tau_{b2}=-1.1\pm1.1$	0.76
τ-7*		2.20±0.01	1.303±0.002	23.1±1	(0.702)	$\tau_{b1}=1.4\pm0.6$ $\tau_{b2}=-1.1\pm0.5$	0.75
τ-8		4.8±0.3	1.139±0.003	30.1±1.4	(0.625)	$\tau_{b1}=0.4\pm0.6$ $\tau_{b2}=-0.2\pm0.5$	0.75
τ-9	(19) +NAC	2.6±3.8	1.30±0.01	26±23	(0.702)	$a_\chi=-1.2\pm9.5$ $\tau_{b1}=1.5\pm2.2$ $\tau_{b2}=-1.2\pm1.7$	0.76

contribution to scattering at temperatures far from T_c. For WBB at $W/S=2$, the typical size of the micelles is 100 Å [26].

The large uncertainties in γ and ν were due to the correlations between the parameters when all the terms were free. Their accuracy was improved by two orders of magnitude when γ or ν was fixed. Fixing $\nu=0.625$ gave $\gamma=1.140\pm0.002$ (fit τ-3), whereas fixing $\gamma=1.24$ gave $\nu=0.6707\pm0.0008$ (fit τ-4). Imposing $\gamma=2\nu$ did not fit the data.

The low value of γ as compared with 2ν may be due to the NAC necessary at large $(T-T_c)$ since the exponent γ was obtained as the limiting slope of the turbidity at large $(T-T_c)$. The fitting function with the NAC is given as

$$\tau=\tau_0(1+t)t^{-\gamma}G(z)(1+a_\chi t^\Delta)+\tau_b \ . \tag{18}$$

The exponent $\Delta=0.5$ is imposed when fitting. Unphysical values were obtained for the exponents when all the terms were free-fitting parameters in Eq. (18). Fixing one of the exponent values (fit τ-5, where ν is fixed at $\nu=0.625$) gave results nearly the same as that for Eq. (17) and $\gamma=1.14$. Therefore the NAC's do not explain the low value of γ. In addition, the scaling relation $\gamma=2\nu$ was never satisfied by the data.

Rouch *et al.* [8] observed a turbidity minimum in the system WDA around $(T_c-T)=10$ K. They interpreted this as a crossover phenomenon from the critical regime $(q_D\xi\gg1)$ of the microemulsion to a merely temperature-dependent regime $(q_D\xi\ll1)$ of a nonideal solution of interacting micelles where q_D^{-1} was typically the size of the micelles. Within the $(T-T_c)$ range that we covered for the present system (30 K), we did not see a minimum in τ. But since the ξ_0 for WBB is 2 times larger than for WDA, the crossover temperature may correspond to a still higher $(T-T_c)$ value [a typical estimate with a micellar size of 100 Å gives $(T-T_c)=42$ K]. Such effects need to be taken into account in analyzing the τ data.

We do not know the exact form of the temperature dependence of the background turbidity. By adding a linear temperature-dependent background turbidity, Eq.

TABLE III. Results of the turbidity fit for sets 3 and 2 of sample B. $\sigma_\tau=0.03$ cm^{-1} for set 2; $\sigma_\tau=0.01$ cm^{-1} for set 3. The $(T-T_c)$ range is 4.3 K for set 3, and the $(T-T_c)$ range is 20 K for set 2.

Set	$10^3(\tau_0\pm\sigma_{\tau_0})$ (cm^{-1})	$\gamma\pm\sigma_\gamma$	$\xi_0\pm\sigma_{\xi_0}$ (Å)	$\nu\pm\sigma_\nu$	As defined (cm^{-1})	χ_ν^2
3	19.4±5.4	0.75±0.07	23.5±1.9	0.49±0.02		0.56
	2.80±0.07	1.265±0.004	20.3±0.7	(0.702)		0.80
2	6.4 ±0.06	1.10±0.03	43.1±0.6	0.57±0.02		4.16
	3.8±1.2	1.225±0.077	36.5±3.1	0.63±0.04	$\tau_b=0.07\pm0.03$	4.17
	1.7±0.13	1.369±0.001	26.4±1.2	(0.702)	$\tau_{b1}=1.86\pm0.7$ $\tau_{b2}=-1.61\pm0.7$	4.17

(17) can be written as

$$\tau=\tau_0(1+t)t^{-\gamma}G(z)+\tau_{b1}+\tau_{b2}(1+t)\ . \qquad (19)$$

By fitting the data by Eq. (19) with all the free terms, we obtained $\nu=0.70\pm0.12$ and $\gamma=1.29\pm0.25$ (fit τ-6 and Fig. 1). The quality of the fit was nearly the same ($\chi_\nu^2=0.76$) as that for the fit τ-2 ($\chi_\nu^2=0.75$).

The uncertainties in the parameters were improved by fixing one of the exponents in Eq. (19). Fits τ-7 and τ-8 correspond to fixing the exponent ν in Eq. (19) and hence were identical except that $\nu=\nu^*=0.702$ in τ-7 and $\nu=0.625$ in τ-8. The χ_ν^2 were the same for the two cases, but the relative standard deviations in the background terms were small when $\nu=\nu^*$. The γ value remained unchanged ($\gamma=1.30$) even when the NAC term was added to Eq. (19) as in the fit τ-9 [27].

Fitting with Eq. (19) gives the Fisher-renormalized value for ν. The γ value so obtained is lower than the Fisher-renormalized value ($\gamma^*=1.39$). This result can be understood when we note that Fisher renormalization of the exponents is complete only in the asymptotic limit [28]. The exponent γ is derived from the turbidity data for large t, whereas ν is from the data at small t. Hence ν is expected to reach its asymptotic value ν^* when γ will lie between the Ising value 1.24 and the Fisher-renormalized value 1.39. Low values of γ have also been observed in other ternary microemulsions in earlier light-scattering studies [3,4,9].

Equations (5) and (6) were also fitted to set 3 of sample B. In this sample, for $(T-T_c)>4$ K, we observed a reproducible height dependence of τ, which we do not understand. Hence the accurate τ data were limited only to 4 K above T_c and were not sufficient to obtain the parameters independently by leaving them free. The expected background turbidity τ_b is around 4% of the turbidity value at T_c [8], which in our case was of the order of 0.1 cm^{-1}. At 4 K above T_c, the measured turbidity for our samples was still 1 cm^{-1} and was much too large to be overdominated by the background effects. Hence

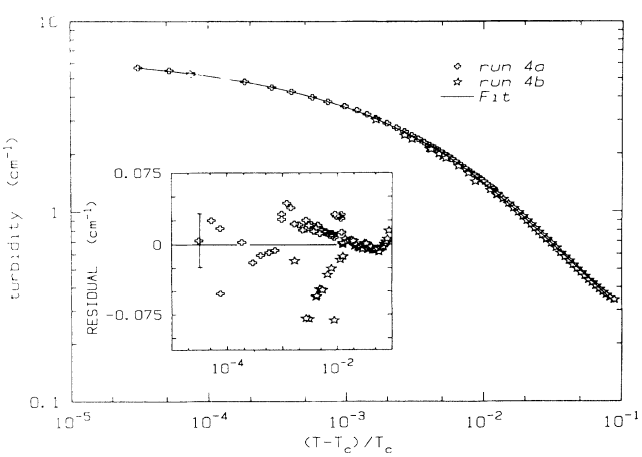

FIG. 1. Turbidity fit with a constant background term and a linear temperature-dependent term in turbidity [Eq. (19) and fit τ-6] for the runs 4a and 4b (A). Inset gives the residuals of the fit. Vertical bar represents one standard deviation.

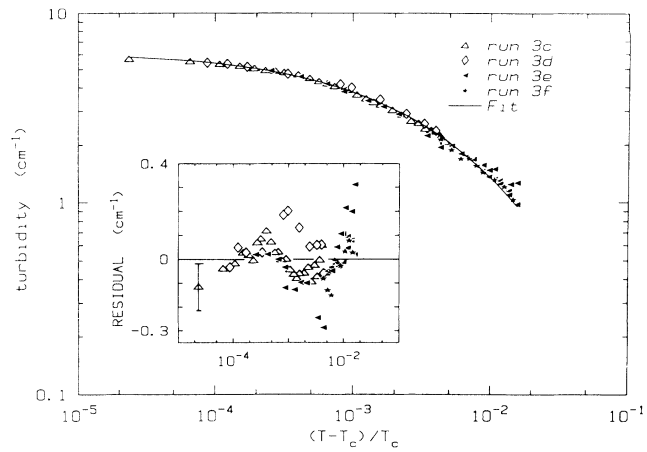

FIG. 2. Turbidity fit with no background term [Eq. (5)] for runs of set 3 (B). The exponent ν is fixed at 0.702 in Eq. (6). Inset gives the residuals of the fit.

we set $\tau_b=0$ for this sample. By fixing $\nu=\nu^*$ and $\tau_b=0$ in Eq. (17), we obtain ξ_0, τ_0, and γ values (Table III), in agreement with the corresponding fits on sample A. The fit is shown in Fig. 2.

The fits from Table II were repeated with set 2 of sample B. As can be seen from Table III, these data are all consistent and agree with the above analysis. However, these data were preliminary and suffered from a larger experimental error. The large χ_ν^2 also is indicative of this.

Although the above discussions show that mere numerical analysis of the turbidity data cannot distinguish between Ising and Fisher-renormalized Ising exponents, physical arguments indicate that the best set of parameters for the turbidity data for WBB are $\nu=0.70$, $\gamma=1.30$, and $\xi_0=23$ Å. The exponent and ξ_0 values for other microemulsion systems (mainly WDA) and theoretical values for the Fisher-renormalized exponents are included in Table IV. The consistency of τ measured from the two independent samples and from cells of different path lengths makes us confident in comparing ρ and n corresponding to the different sets of the same samples.

TABLE IV. Comparison of literature values of γ, ν, and ξ_0 for various systems with the present system (WBB) and theory. $(T-T_c)/T_c$ is the variable unless mentioned.

Reference	System	γ	ν	ξ_0 (Å)
[3(a)]	WDA[b]	1.22	0.75	12.2
[4] sample 1	WDA[b]	1.30	0.76	7.2
[4] sample 2	WDA[b]	1.25	0.71	9.3
[9]	WDPH[a,b]	1.21	0.66	
[3(b)]	WDA[c]	1.61	0.72	11
[3(c)]	WDA[d]	1.5	0.7	
Our result	WBB	1.303	0.70	23
Theory		1.393	0.702	

[a]WDPH: water+decane+potassium oleate+hexanol.
[b]Light scattering.
[c]Neutron-scattering result.
[d]Pressure as the variable.

B. Density and refractive index

The raw data are given in Fig. 3(a) for the density and in Fig. 4(a) for the refractive index. From the Introduction we see that both ρ and n can be described by the scaling form

$$Y=a_c^i+[a_1T_c^it+a_2(T_c^it)^2+a_3(T_c^it)^3+\cdots]+a_Y(T_c^it)^{(1-\alpha)}[1+a_{Y_1}(T_c^it)^{\Delta}+\cdots]\ . \tag{20}$$

Y stands for ρ or n. The i index here represents a run. a_1, a_2, a_3 are the amplitudes of the background terms, a_Y is the amplitude of the critical term, and a_{Y_1} is the first NAC.

The results of the analysis of the density data for sets 1 and 2 of sample B and set 4 of sample A are given in Table V. a_c^i is the critical density for ρ and shows a set dependence, and the differences are within the absolute accuracy of ρ. For simplicity of presentation, only the average of a_c^i over i is given. The data were well described by linear plus quadratic terms (LF+QF) in Eq. (20). Least-squares fits were also performed with the linear and the $(1-\alpha)$ terms (LF+PF) and linear, quadratic, and $(1-\alpha)$ terms (LF+QF+PF) in Eq. (20), where $(1-\alpha)=0.89$ is fixed. Comparing the parameter uncertainties and the χ_ν^2 between these four fits, we judge that the fit LF+QF [Fig. 3(b)] is the best. The same data in a small temperature range of 3.5 K showed preference to LF+PF with a large uncertainty on a_Y. However, from the residual plot for the linear fit [Fig. 3(c)], we see that, within the standard deviations of the data, the residuals are random for LF.

For sample A the density data were available in a temperature range of 3.5 K only. All the fits described above for sample B were repeated. Using the same criteria discussed above, we judged that the fit LF was the best. The residual plot for LF is shown in Fig. 3(d).

The refractive-index data from set 3 of sample B was fitted by a polynomial function up to degree 2 (LF+QF). The residuals showed a systematic negative deviation of the order of the precision of n [Fig. (4b)], indicating that there is a very weak anomaly. To take into account this anomaly in the analysis, we added (i) a power-law term as in Eq. (20) with the exponent fixed at 0.89, leading to the fit LF+QF+PF, and (ii) an exponential term from Ref. [10], leading to the fit LF+QF+EF, as shown by

$$n=a_c^i+[a_1T_c^it+a_2(T_c^it)^2]-10^{-6}\exp\left[\frac{D}{1+t}-Et\right]\ . \tag{21}$$

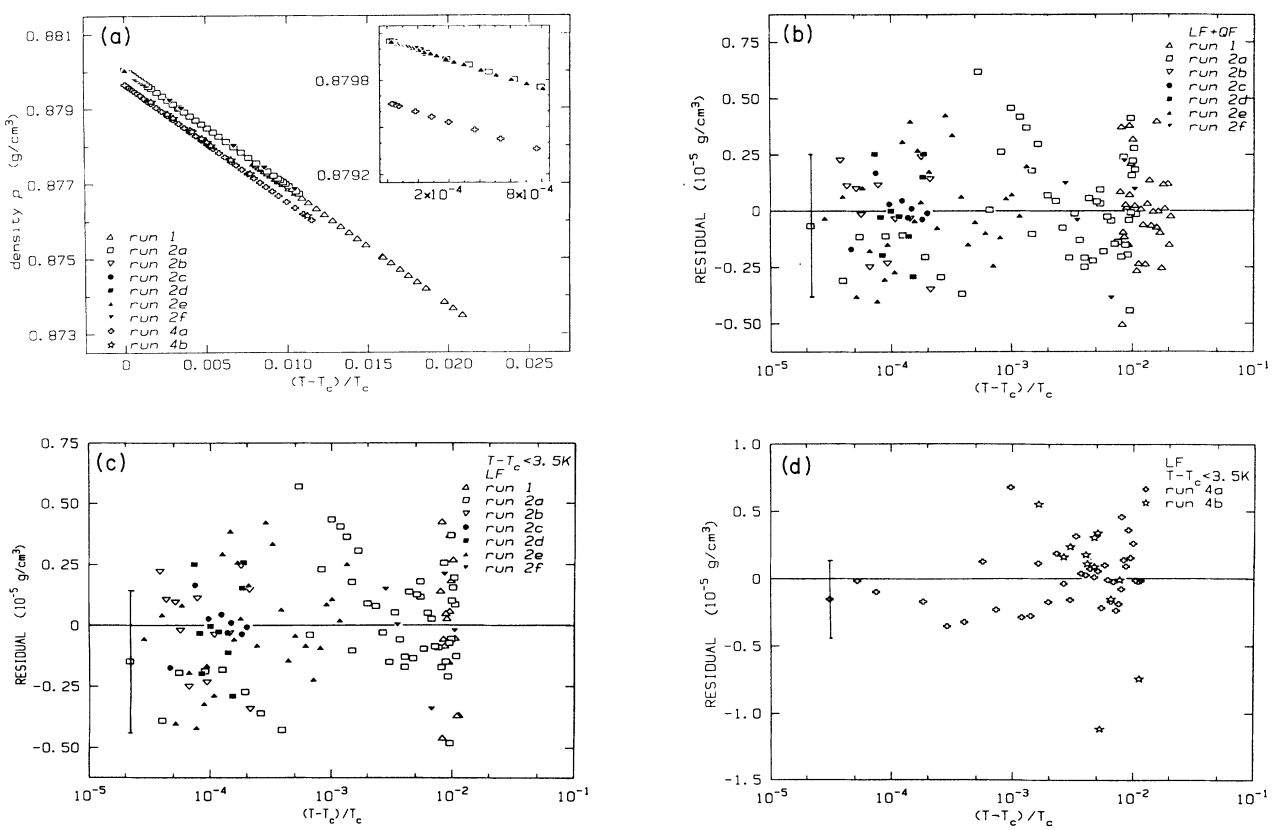

FIG. 3. Temperature variation of the density: (a) Experimental (A+B) data. A constant of 0.003 for runs 4a,4b and 0.0004 for run 1 are added to the density values for display purposes. Inset shows the raw data within 300 mK close to T_c. (b), (c) residual plots for sample B: (b) LF+QF for the full $(T-T_c)$ range, (c) LF for the $(T-T_c)$ range of 3.5 K. (d) residual plot for sample A for LF in the $(T-T_c)$ range of 3.5 K.

TABLE V. Results of the fit to Eq. (20) for density for samples B and A. $1-\alpha=0.89$; $\sigma_\rho=\pm3\times10^{-6}$ g cm^{-3}. An asterisk indicates the fit we judge the best. T_r is the temperature range of data above T_c.

Sample (set)	T_r (K)	Fit	$10^6(a_c\pm\sigma_{ac})$ (g cm^{-3})	$10^4(a_1\pm\sigma_{a1})$ (g cm^{-3} K^{-1})	$10^7(a_2\pm\sigma_{a2})$ (g cm^{-3} K^{-2})	$10^4(a_y\pm\sigma_{aY})$	χ_ν^2
B(1,2)	6.3	LF	880 000±1	−10.364±0.003			0.77
		LF+QF*	879 999±1	−10.326±0.007	−7.06±0.10		0.46
		LF+PF	879 997.0±1.1	−10.62±0.04		0.31±0.05	0.48
		LF+QF+PF	879 998.0±1.2	−10.41±0.14	−5.1±3.4	0.09±0.15	0.47
	3.5	LF*	879 999±1	−10.348±0.004			0.48
		LF+QF	879 999±1	−10.334±0.014	−4.5±4.1		0.48
		LF+PF	879 998.0±1.1	−10.48±0.08		0.16±0.09	0.46
		LF+QF+PF	879 998.0±1.3	−10.8±0.3	16±12	0.48±0.26	0.41
A(4)	3.5	LF*	876 687±1	−10.368±0.004			0.91
		LF+QF	876 686.0±1.5	−10.35±0.015	−5.0±4.5		0.90
		LF+PF	876 685.0±1.5	−10.498±0.090		0.15±0.11	0.98
		LF+QF+PF	876 685.0±1.9	−10.7±0.4	7.0±4.4	0.32±0.36	0.90

The results are presented in Table VI. Since starting values of the fringe order were arbitrary, a_c^i represents an arbitrary number, the intercept at $t=0$ for the run i. For sake of simplicity, a_c^i values were not included in the Table VI. The value of χ_ν^2 was better for the fit LF+QF+EF with smaller uncertainties in the parameters than for the fit LF+QF+PF. The residuals are shown in Fig. 4(c). Also note that the linear coefficient (a_1) for the fit LF+QF+EF corresponds to that from fits LF and LF+QF, whereas it is much larger for the fit LF+QF+PF and is unphysical.

The fits described above for the full-range refractive-index were repeated for the data with $(T-T_c)<3.5$ K without the quadratic term in the exponential and power-law fits. The fit LF+EF remains slightly better than the other fits [Table VI and Fig. 4(d)]. This suggests

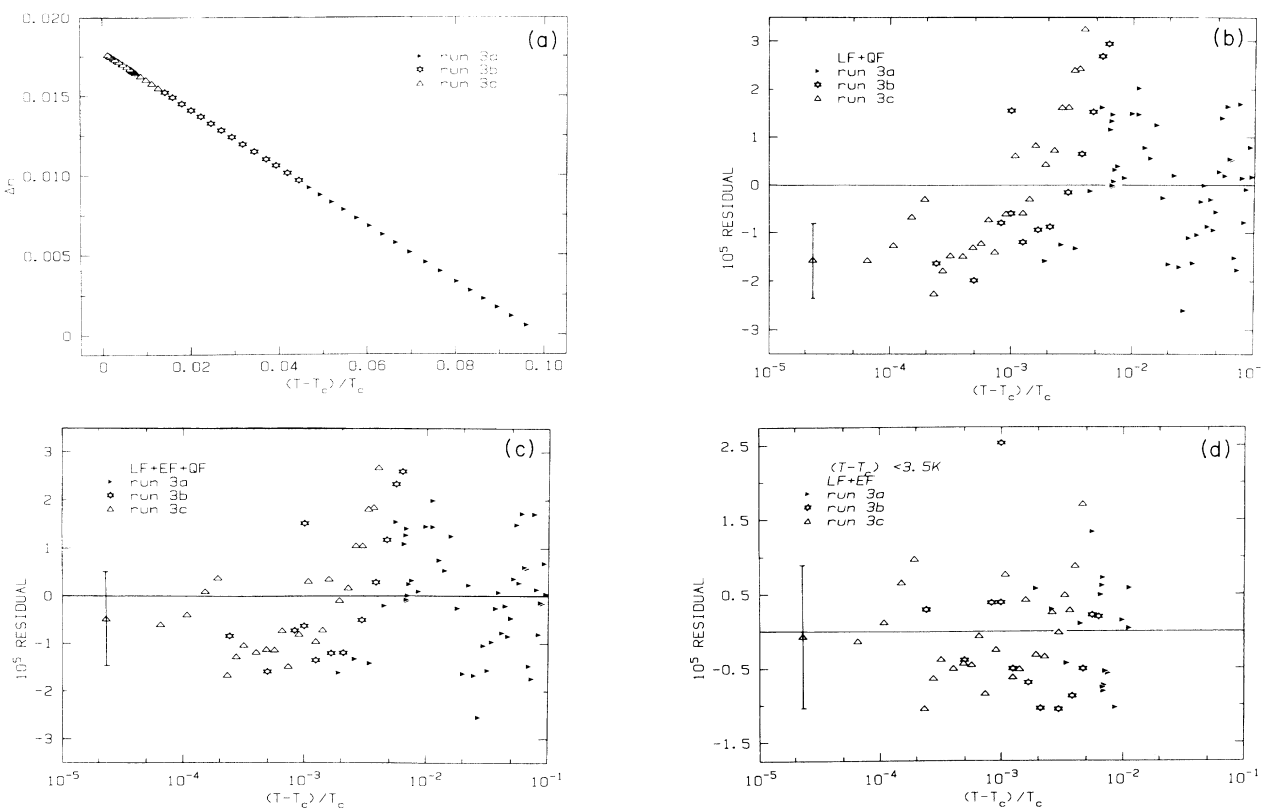

FIG. 4. Temperature variation of the refractive index for set 3 of sample B. (a) Experimental data. (b), (c) residual plots for data in the full $(T-T_c)$ range: (b) quadratic fit (LF+QF), (c) exponential fit [Eq. (21) and fit LF+QF+EF]. (d) residual plot in the $(T-T_c)$ range of 3.5 K for an exponential fit (LF+EF).

TABLE VI. Results of the refractive-index fits to Eqs. (20) and (21) for the set 3 of sample B. $\sigma_n = \pm 1.0 \times 10^{-5}$. An asterisk indicates the fit we judge the best.

Fit	Range $T-T_c<T_r$ T_r K	$10^4(a_1 \pm \sigma_{a1})$ (K^{-1})	$10^7(a_2 \pm \sigma_{a2})$ (K^{-2})	$10^4(a_Y \pm \sigma_{aY})$[a]	χ_ν^2
LF	28.7	-6.045 ± 0.002			20.89
LF+QF		-6.290 ± 0.006	9.3 ± 0.2		1.97
LF+QF+PF		-7.22 ± 0.12	13.6 ± 0.6	1.19 ± 0.15	1.26
LF+QF+EF*		-6.32 ± 0.01	10.1 ± 0.3	$D = 1217 \pm 40$ $E = 336 \pm 84$	0.88
LF	3.5	-6.060 ± 0.002			0.83
LF+QF		-5.897 ± 0.050	57.7 ± 15.7		0.59
LF+PF		-7.17 ± 0.31		1.26 ± 0.35	0.60
LF+EF*		-6.26 ± 0.25		$D = 1255 \pm 486$ $E = 198 \pm 290$	0.58

[a]Unless defined.

that the exponential function describes the observed weak anomaly best and rules out an intrinsic anomaly of the $(1-\alpha)$ type in n for these samples. Since set 5 of sample A was noncritical, we do not present the n data for sample A.

The linear temperature coefficient from the best fit for density agrees within 3×10^{-6} between samples B and A, which is within the relative precision of the density data, and $(d\rho/dT)_{\text{expt}}$ is $(-1.033 \pm 0.007) \times 10^{-3}$ g cm^{-3} K^{-1}. The literature values for the pure components at 30 °C are $\rho_{\text{benzene}} = 0.8681$ g cm^{-3}, $(d\rho/dT)_{\text{benzene}} = -1.0636 \times 10^{-3}$ g cm^{-3} K^{-1} and $\rho_{\text{water}} = 0.9956$ g cm^{-3}, $(d\rho/dT)_{\text{water}} = -0.306 \times 10^{-3}$ g cm^{-3} K^{-1} respectively [29]. This gives $(d\rho/dT)_{\text{calc}} = -0.9952 \times 10^{-3}$ g cm^{-3} K^{-1} for the microemulsion sample B using the experimental value for the microemulsion density at 30 °C (0.8774 g cm^{-3}) and assuming volume additivity. The contributions from the surfactant are ignored.

The linear temperature coefficient from the best fit for the refractive index is $(dn/dT)_{\text{expt}} = (-6.32 \pm 0.01) \times 10^{-4}$/K. The literature data for the pure components at 30 °C and $\lambda = 633$ nm are $n_{\text{benzene}} = 1.4949$, $(dn/dT)_{\text{benzene}} = (-6.523 \times 10^{-4})$/K [19] and $n_{\text{water}} = 1.3288$, $(dn/dT)_{\text{water}} = -1.23 \times 10^{-4}$/K [29,30]. The refractive index of the microemulsion sample B calculated from the pure component values through the LL formula, using the experimental value for the microemulsion density and assuming $n_{\text{BHDC}} = n_{\text{benzene}}$, is 1.4875. This is in agreement with the measured value of 1.486 ± 0.001 at 30 °C using an Abbe refractometer. The (dn/dT) value is calculated from the LL formula using the experimental values of ρ, $d\rho/dT$, and n: $(dn/dT)_{\text{LL}} = (-6.71 \pm 0.07) \times 10^{-4}$/K. This value is approximately 6% more than the experimentally measured dn/dT. This is within the expected correction in noncritical fluids [19].

V. CONCLUSION

A detailed study of the ternary microemulsion WBB clearly shows its Ising behavior. The expected Fisher renormalization of the exponent values for the thermodynamic path considered here does not come out unambiguously from mere numerical analysis. However, the physical arguments relevant to these systems suggest that the obtained exponent values for the correlation length and osmotic susceptibility and the absence of the density anomaly are in accord with the Fisher-renormalized Ising behavior. The observed weak anomaly in the refractive index is independent both of the density behavior and of the $(1-\alpha)$ behavior expected as an intrinsic critical contribution to n in Ising systems. On the other hand, this anomaly is consistent with the model discussed for the quaternary microemulsion WDSP [5] near a CEP. This suggests that the n anomaly may be the remnant of a CEP, leading to a different micellar organization. It is interesting to recall that for the well-studied ternary microemulsion WDA the critical points close to the CEP and far off from the CEP have shown similar critical behavior [4], unlike in the quaternary system WDSP [5]. The difference in the critical behavior between the microemulsions WDSP and WDA is believed to be due to the fact that the compositions of the coexisting microemulsion and sponge phases were very close to each other in WDSP, whereas they were widely different in WDA [1]. Hence, in WDSP, one could have the precursor fluctuations of the sponge phase before the phase separation near CEP, leading to deviations to Ising behavior. In addition, the presence of a tricritical point along the thermodynamic paths to ordinary critical points is shown to give effective values for the critical exponents in WDSP [31]. In the absence of the knowledge of the complete phase diagram for the present system WBB, it is difficult to assign a precise origin to the weak anomaly in n.

ACKNOWLEDGMENTS

We are grateful to J. R. Lalanne and N. Rebbouh for providing us with the microemulsion samples and for discussions and suggestions on the manuscript. We acknowledge the assistance of F. Perrot during the experimentation. We thank G. Zalczer for a critical reading of the manuscript. Discussions with C. Bervillier and C. Bagnuls were very fruitful, and we thank them.

[1] A. M. Bellocq and D. Roux, in *Microemulsions: Structure and Dynamics,* edited by S. E. Friberg and P. Bothorel (CRC, Boca Raton, FL, 1987), Chap. 2.
[2] C. Bagnuls and C. Bervillier, Phys. Rev. Lett. **58**, 435 (1987), and references therein.
[3] (a) J. S. Huang and M. W. Kim, Phys. Rev. Lett. **47**, 1462 (1981); (b) M. Kotlarchyk, S. H. Chen, and J. S. Huang, Phys. Rev. A **28**, 508 (1983); (c) M. W. Kim, J. Bock, and J. S. Huang, Phys. Rev. Lett. **54**, 46 (1985).
[4] P. Honorat, D. Roux, and A. M. Bellocq, J. Phys. (Paris) Lett. **45**, L961 (1984).
[5] A. M. Bellocq, P. Honorat, and D. Roux, J. Phys. (Paris) **46**, 743 (1985).
[6] N. Rebbouh and J. R. Lalanne, J. Chem. Phys. **90**, 1175 (1989).
[7] C. Pepin, T. K. Bose, and J. Thoen, Phys. Rev. A **39**, 835 (1989); S. C. Greer, T. K. Bose, and J. Thoen, J. Chem. Phys. **91**, 620 (1989).
[8] J. Rouch, A. Safouane, P. Tartaglia, and S. H. Chen, J. Chem. Phys. **90**, 3756 (1989).
[9] G. Maisano, F. Mallamace, and N. Micali, Phys. Rev. A **39**, 4103 (1989).
[10] N. Rebbouh, D. Beysens, and J. R. Lalanne, J. Chem. Phys. **93**, 9026 (1990).
[11] R. B. Griffiths and J. C. Wheeler, Phys. Rev. A **2**, 1047 (1970).
[12] M. E. Fisher, Phys. Rev. **176**, 257 (1968).
[13] C. Pepin, T. K. Bose, and J. Thoen, Phys. Rev. Lett. **60**, 2507 (1988).
[14] D. Beysens and G. Zalczer, Europhys Lett. **8**, 777 (1989).
[15] D. Beysens and G. Zalczer, Phys. Rev. Lett. **65**, 1690 (1990); T. K. Bose, *ibid.* **65**, 1691 (1990).
[16] V. G. Puglielli and N. C. Ford, Phys. Rev. Lett. **25**, 143 (1970).
[17] D. Beysens and G. Zalczer, J. Chem. Phys. **92**, 6747 (1990).
[18] J. Yvon, C. R. Acad. Sci. **292**, 35 (1936); J. G. Kirkwood, J. Chem. Phys. **4**, 592 (1936).
[19] D. Beysens and P. Calmettes, J. Chem. Phys. **66**, 766 (1977).
[20] R. Hocken and G. Stell, Phys. Rev. A **8**, 887 (1973).
[21] Sample A was supplied by Professor J. R. Lalanne, C. N. R. S., Centre de Recherche Paul Pascal, Pessac, France, and sample B was supplied by Dr. N. Rebbouh, G. R. D., Physique, Université du Québec à Trois Rivières, Québec, Canada.
[22] The raw data are not presented because of the large number of data points. They can be obtained on request.
[23] D. Beysens, Rev. Sci. Instrum. **15**, 509 (1979).
[24] P. Guenoun, R. Gastaud, F. Perrot, and D. Beysens, Phys. Rev. A **36**, 4876 (1987).
[25] (a) P. R. Bevington, *Data Reduction and Error Analysis for the Physical Sciences* (McGraw-Hill, New York, 1969); (b) C. Shetty, M. K. Gunasekaran, V. Vani, and E. S. R. Gopal, Pramana **21**, 71 (1983).
[26] D. Chatenay, W. Urbach, A. M. Cazabat, and D. Langevin, Phys. Rev. Lett. **54**, 2253 (1985).
[27] Since Fisher renormalization of exponents is effective only close to T_c, when fixing the value of Δ in the fits, its value should be $\Delta=0.5$ and not $\Delta=\Delta^*=\Delta/(1-\alpha)=0.56$. However, we found that the difference between the two values hardly affects the fits and parameter values.
[28] M. E. Fisher and P. E. Scesney, Phys. Rev. A **2**, 825 (1970).
[29] *International Critical Tables* (McGraw-Hill, New York, 1933).
[30] Y. Jayalakshmi, J. S. van Duijneveldt, and D. Beysens (unpublished).
[31] D. Gazeau, E. Freysz, and A. M. Bellocq, Europhys. Lett. **9**, 833 (1989).